Trehalose supports the growth of *Aedes aegypti* cells and modifies gene expression and dengue virus replication

Andrew D. Marten[1], Douglas P. Haslitt[1], Chad A. Martin[1], Daniel H. Swanson[2], Karishma Kalera[2,3], Ulysses G. Johnson[2,3], Benjamin M. Swarts[2,3], and Michael J. Conway[1]

[1]*Foundational Sciences, Central Michigan University College of Medicine, Mount Pleasant, MI 48859, USA.*

[2]*Department of Chemistry and Biochemistry, Central Michigan University, Mount Pleasant, MI 48859, USA.*

[3]*Biochemistry, Cell, and Molecular Biology Graduate Programs, Central Michigan University, Mount Pleasant, MI 48859, USA.*

Address correspondence to: Foundational Sciences, Central Michigan University College of Medicine, Mount Pleasant, MI, 48859

E-mail: michael.conway@cmich.edu. Phone: (989) 774-3930, Fax: (989) 774-3462

Short title: Trehalose metabolism in *Aedes aegypti*

Abstract

Trehalose is a non-reducing disaccharide that is the major sugar found in insect hemolymph fluid. Trehalose provides energy, and promotes growth, metamorphosis, stress recovery, chitin synthesis, and insect flight. Trehalase is the only enzyme responsible for the hydrolysis of trehalose, which makes it an attractive molecular target. Here we show that *Aedes aegypti* (Aag2) cells express trehalase and that they can grow on trehalose-containing cell culture media. Trehalase activity was confirmed by treating Aag2 cells with trehalase inhibitors, which inhibited conversion of trehalose to glucose and reduced cell proliferation. Cell entry of a fluorescent trehalose probe was dependent on trehalose concentration, suggesting that trehalose moves across the cell membrane via passive transport. Culturing Aag2 cells with trehalose-containing cell culture media led to significant changes in gene expression, intracellular lipids, and dengue virus replication and specific infectivity, and increased their susceptibility to trehalase inhibitors. These data describe an *in vitro* model that can be used to rapidly screen novel trehalase inhibitors and probes and underscores the importance of trehalose metabolism in *Ae. aegypti* physiology and transmission of a mosquito-borne virus.

55 **Introduction**

56 *Aedes aegypti* is the primary vector of several important global human pathogens
57 including dengue virus (DENV), Zika virus (ZIKV), and chikungunya virus (CHIKV).
58 There are no targeted antivirals for these viruses and the currently licensed DENV vaccine
59 is restricted to a subset of the human population due to the potential of eliciting antibody-
60 dependent enhancement (ADE) in those who have not previously been infected (1-6).
61 Further, resistance to pesticides including carbamates, organochlorines, organophosphates,
62 and pyrethroids has been detected in the Americas, Africa, and Asia. New strategies to
63 control disease vectors are desperately needed (7-13).

64

65 Trehalose is a non-reducing disaccharide and is the most prevalent sugar found in
66 insect hemolymph fluid. Trehalose provides energy but also promotes growth,
67 metamorphosis, stress recovery, chitin synthesis, and insect flight (14-28). Previous
68 research has shown that trehalose is synthesized in the insect fat body from glucose 6-
69 phosphate and UDP-glucose by the conserved enzymes trehalose 6-phosphate synthase
70 (TPS) and trehalose 6-phosphate phosphatase (TPP) (16, 22, 29, 30). The hydrolysis of
71 trehalose is under the enzymatic control of trehalase, which catalyzes the conversion of
72 trehalose into two glucose molecules (22, 30). There are two forms of insect trehalase.
73 Trehalase 1 (Tre-1) is soluble and has been purified from hemolymph, midgut goblet cells,
74 and eggs. Trehalase 2 (Tre-2) is a membrane bound form and has been identified in flight
75 muscle, follicle cells, ovary cells, spermatophore, midgut, and brain tissue (22). Although
76 it is known that the facilitated trehalose transporter (TRET1) transfers newly synthesized

77 trehalose from the fat body across the cellular membrane and into the hemolymph, it is
78 unclear if trehalose transporters exist in peripheral tissues and import this sugar (22).
79
80 Trehalose is not synthesized by human cells, but it is present in varying quantities
81 in certain foods such as mushrooms, yeast, honey, beans, seaweeds, and shellfish, and
82 synthesized by certain bacterial species that comprise the microbiome (31). Humans
83 express a membrane-bound trehalase enzyme in the small intestine's brush border cells,
84 which catalyzes dietary trehalose to glucose (31). Mammalian cells do not normally engage
85 with high concentrations of trehalose, and previous research indicates that treatment of
86 mammalian cells with trehalose induces autophagy through an MTOR-independent
87 mechanism. This has been associated with both neuroprotective and antiviral activities (32-
88 39).
89
90 Our previous research revealed that treatment of *Ae. aegypti* with the trehalase
91 inhibitor validamycin A (ValA) promoted hypoglycemia and trehalose accumulation, and
92 corresponded with delayed larval and pupal development, ultimately preventing flight in
93 adult mosquitoes (23). Unfortunately, a novel trehalose analogue called 5-ThioTre was
94 unable to recapitulate the activity of ValA (23). We sought to develop an *in vitro* model
95 that would facilitate screening of novel trehalose analogues and to determine the impact of
96 trehalose metabolism on a mosquito-borne virus. Here, we show that the *Ae. aegypti* cell
97 line (Aag2) expresses a secreted trehalase isoform, and that this enzyme facilitates growth
98 when cell culture media glucose is exchanged for trehalose. Specifically, the trehalase
99 inhibitor validamycin A (ValA) and novel trehalase inhibitors prevented conversion of cell

100 culture media trehalose to glucose, and treatment with ValA significantly reduced cell
101 proliferation. Cell entry of a fluorescent trehalose probe was dependent on trehalose
102 concentration, suggesting that trehalose moves across the cell membrane via passive
103 transport. Importantly, RNA-Seq analysis of Aag2 cells grown in trehalose-containing cell
104 culture media revealed significant changes in gene expression in multiple cellular
105 pathways, including those involved in integral/intrinsic membrane components. Trehalose
106 also increased the concentration of intracellular lipids and viral RNA (vRNA), shedding of
107 infectious virus, and the specific infectivity of DENV virions, while increasing the
108 susceptibility of Aag2 cells and DENV to trehalase inhibitors. This manuscript describes
109 the use of an *in vitro* model that can be used to interrogate trehalose metabolism in insect
110 cells and reveals how trehalose modulates mosquito cell biology and virus infection.
111

112 **Methods**

113

114 **Cells and reagents.** The *Ae. aegypti* cell line, Aag2 (ATCC, VA), was used for *in vitro*
115 studies. Aag2 cells were maintained at 28 °C with 5% CO2 in complete cell culture media
116 containing DMEM no glucose media supplemented with 4,500 mg/L glucose, 10% heat-
117 inactivated fetal bovine serum (FBS) (Gemini, CA), 1% penicillin-streptomycin (Thermo
118 Fisher Scientific, MA) and 1% tryptose phosphate broth (Sigma-Aldrich, MO). Aag2 cells
119 were also grown using the above cell culture media with equimolar concentrations of
120 trehalose (2,250 mg/L) (Sigma-Aldrich, MO) instead of glucose. It is important to note that
121 the trehalose-containing cell culture media retained low concentrations of glucose from
122 FBS and tryptose phosphate broth. The glucose concentration in our trehalose-containing

123 cell culture media was approximately 125 mg/L but rapidly increased in glucose
124 concentration after inoculation onto Aag2 cells. The virus strain used was dengue virus
125 type 2 New Guinea C (DENV2 NGC). DENV2 stocks were made by infecting Aag2 cells
126 at a MOI of 1.0 and cell-free virus stocks were harvested 8 days post-infection (dpi) and
127 stored at −80 °C until use.
128
129 **Trehalose analogues.** Validamycin A (ValA) (Cayman Chemical, MI) was the only
130 commercially available trehalase inhibitor available at the time of this study. The synthesis
131 of trehalose analogues was carried out using a chemoenzymatic method as previously
132 reported for 5-ThioTre (40) and 6-$TreNH_2$ (41). The water solubility of 5-ThioTre and 6-
133 $TreNH_2$ is predicted to be very close to trehalose and stocks were generated in water at 100
134 mM.
135
136 **Synthesis of fluorescent trehalose derivative NBD-Trehalose.** To a 25 mL round bottom
137 flask flushed under argon was added anhydrous *N*,*N*-dimethylformamide (10 mL), 6-
138 $TreNH_2$ (10.9 mg, 0.032 mmol), 4-chloro-7-nitrobenzo-2-oxa-1,3-diazole (7.6 mg, 0.038
139 mmol), and *N*,*N*-diisopropylethylamine (8 μL, 0.043 mmol). After stirring at room
140 temperature under argon overnight, thin-layer chromatography indicated that the reaction
141 was complete. The crude product was concentrated by rotary evaporation and purified by
142 reverse phase chromatography on a Biotage Isolera One automated flash chromatography
143 system (10 g C18 column; 0% CH_3CN in H_2O → 80% CH_3CN in H_2O) to give NBD-
144 Trehalose (12.9 mg, 80%) as an orange solid. ^1H NMR (500 MHz, D_2O): δ 8.38 (d, J = 9.0
145 Hz, 1 H), 6.38 (d, J = 9.0 Hz, 1 H), 5.18 (d, J = 4.0 Hz, 1 H), 5.06 (d, J = 3.5 Hz, 1 H),

146 4.11-4.07 (m, 1 H), 3.94 (bs, 1 H), 3.87-3.76 (m, 5 H), 3.71 (dd, *J* = 5.5, 12.0 Hz, 1 H),
147 3.67 (dd, *J* = 4.0, 10.0 Hz, 1 H), 3.47 (t, *J* = 10.0 Hz, 1 H), 3.46 (dd, *J* = 3.5, 10.0 Hz, 1 H),
148 3.38 (t, *J* = 10.0 Hz, 1 H). ^{13}C NMR (125.7 MHz, D_2O): δ 146.46, 144.32, 143.82, 120.62,
149 138.70, 100.64, 93.47, 93.33, 72.58, 72.51, 71.17, 71.34, 70.93, 70.89, 70.51, 69.61, 60.49,
150 48.59. HRMS (ESI-TOF) m/z: $[M + Na]^+$ Calcd for $C_{18}H_{24}N_4O_{13}Na$ 527.1238; Found
151 527.1249. Stocks of NBD-Trehalose were generated in dimethylsulfoxide (DMSO) at 100
152 mM.
153
154 **Cell proliferation and glucose assays.** Cell proliferation assays were performed by
155 seeding 100 Aag2 cells into a 96 well plate in triplicate. The total number of viable cells
156 per well were quantified using trypan blue exclusion each day starting on day 0 and ending
157 on day 7. This assay was repeated using cells that were fed either glucose or trehalose-
158 containing cell culture media in the presence or absence of 1 mM validamycin A (ValA).
159 A Glucose Colorimetric Assay Kit (Cayman Chemical, MI) was used to assay glucose
160 concentration in Aag2 cell-free supernatant from cells grown in either glucose or trehalose-
161 containing cell culture media each day starting on day 0 and ending on day 3. Glucose
162 concentration was also assayed in Aag2 cell-free supernatant from cells grown in trehalose-
163 containing cell culture media and in the presence of increasing concentrations of ValA, and
164 trehalose analogues 5-ThioTre and 6-TreNH2, which are described above. Glucose
165 concentration was also assayed in Aag2 cell-free supernatant from cells that were infected
166 with 1 MOI DENV2 every other day starting 1-day post-infection (dpi) and ending 7 dpi.
167

168 **NBD-Tre probe assays.** Aag2 cells were grown to confluence in trehalose-containing cell
169 culture media using the Nunc Lab-Tek Chamber Slide System (Thermo Fisher Scientific,
170 MA). Cell culture media was removed and replaced with cell culture media spiked with
171 0.1 mM NBD-Tre probe with and without 1 mM ValA. Negative controls included wells
172 treated with equimolar concentrations of the DMSO vehicle control. Treated cells were
173 incubated for 4 hours, cell culture media was then removed, and cells were stained with
174 the nuclear stain Hoescht (Thermo Fisher Scientific, MA). Cells were imaged immediately
175 using a Leica DM5000 B, Leica DFC550 digital camera, and Leica CTR5000 control unit.
176 Mean fluorescence intensity (MFI) per cell was quantified using ImageJ and included 10
177 separate images per condition and the average MFI of 5 cells per image. This experiment
178 was repeated by treating Aag2 cells with 0.1 mM NBD-Tre probe in the presence of
179 increasing concentrations of glucose or trehalose and on uninfected and DENV2-infected
180 cells.
181
182 **Nile Red assay.** Aag2 cells were grown to confluence in either glucose or trehalose-
183 containing cell culture media using the Nunc Lab-Tek Chamber Slide System. A 30 mM
184 Nile Red (Cayman Chemical, MI) stock in DMSO was diluted 1:3000 in either glucose or
185 trehalose-containing cell culture medium and incubated for 30 minutes at room
186 temperature. Cells were fixed and counterstained with the nuclear stain Hoescht. Cells were
187 imaged immediately using a Leica DM5000 B, Leica DFC550 digital camera, and Leica
188 CTR5000 control unit. Corrected total cell fluorescence (CTCF) was quantified using
189 integrated density, area, and mean background fluorescence data obtained from 3 separate
190 images per condition and 20 cells per image.

191

192 **RNA-Seq.** RNA Sequencing (RNASeq) was conducted using a service offered by
193 Novogene, USA (California UC Davis) on Aag2 cells that were either maintained in
194 glucose or trehalose-containing cell culture media in triplicate. RNA was extracted using
195 the Qiagen RNeasy Plus RNA Extraction kit with gDNA eliminator columns. RNA
196 integrity was assessed using the RNA Nano 6000 Assay Kit of the Bioanalyzer 2100
197 system (Agilent Technologies, CA, USA). Total RNA was used as input material for the
198 RNA sample preparations. Briefly, mRNA was purified from total RNA using poly-T
199 oligo-attached magnetic beads. Fragmentation was carried out using divalent cations under
200 elevated temperature in First Strand Synthesis Reaction Buffer(5X). First strand cDNA
201 was synthesized using random hexamer primer and M-MuLV Reverse
202 Transcriptase(RNase H-). Second strand cDNA synthesis was subsequently performed
203 using DNA Polymerase I and RNase H. Remaining overhangs were converted into blunt
204 ends via exonuclease/polymerase activities. After adenylation of 3' ends of DNA
205 fragments, Adaptor with hairpin loop structure were ligated to prepare for hybridization.
206 In order to select cDNA fragments of preferentially 370~420 bp in length, the library
207 fragments were purified with AMPure XP system (Beckman Coulter, Beverly, USA). Then
208 PCR was performed with Phusion High-Fidelity DNA polymerase, Universal PCR primers
209 and Index (X) Primer. At last, PCR products were purified (AMPure XP system) and
210 library quality was assessed on the Agilent Bioanalyzer 2100 system. The clustering of the
211 index-coded samples was performed on a cBot Cluster Generation System using TruSeq
212 PE Cluster Kit v3-cBot-HS (Illumia) according to the manufacturer's instructions. After
213 cluster generation, the library preparations were sequenced on an Illumina Novaseq

platform and 150 bp paired-end reads were generated. Raw data (raw reads) of fastq format were firstly processed through in-house perl scripts. In this step, clean data (clean reads) were obtained by removing reads containing adapter, reads containing ploy-N and low-quality reads from raw data. At the same time, Q20, Q30 and GC content the clean data were calculated. All the downstream analyses were based on the clean data with high quality. Reference genome and gene model annotation files were downloaded from genome website directly. Index of the reference genome was built using Hisat2 v2.0.5 and paired-end clean reads were aligned to the reference genome using Hisat2 v2.0.5. We selected Hisat2 as the mapping tool for that Hisat2 can generate a database of splice junctions based on the gene model annotation file and thus a better mapping result than other non-splice mapping tools. featureCounts v1.5.0-p3 was used to count the reads numbers mapped to each gene. FPKM of each gene was calculated based on the length of the gene and reads count mapped to this gene. FPKM, expected number of Fragments Per Kilobase of transcript sequence per Millions base pairs sequenced, considers the effect of sequencing depth and gene length for the reads count at the same time, and is currently the most commonly used method for estimating gene expression levels. Differential expression analysis of the two conditions/groups was performed using the DESeq2 R package (1.20.0). DESeq2 provide statistical routines for determining differential expression in digital gene expression data using a model based on the negative binomial distribution. The resulting P-values were adjusted using the Benjamini and Hochberg's approach for controlling the false discovery rate. Genes with an adjusted P-value < = 0.05 found by DESeq2 were assigned as differentially expressed. Functional annotations of differentially expressed genes were performed using the g:Cost Functional Profiling tool at g:Profiler and NCBI's

237 DAVID Functional Annotation Bioinformatics tool. FASTQ files for each sample are
238 available in the NCBI SRA database (BioProject ID: PRJNA936836 and PRJNA882813).
239
240 **Focus-forming unit assays.** Aag2 cells were seeded into 96 well plates and grown to ~70%
241 confluence in glucose-containing cell culture media. Wells were then inoculated with 20
242 focus-forming units (FFUs) of DENV2 in either glucose or trehalose-containing cell
243 culture media for 1 hour at 27°C. Unbound virus was removed and fresh glucose-
244 containing cell culture media was added. At 3 dpi, confluent Aag2 monolayers were fixed
245 in 4% paraformaldehyde in phosphate buffered saline (PBS) for 10 minutes, cell
246 membranes were permeabilized with 0.1% Triton X-100, and DENV2 antigen was stained
247 with 1:200 anti-DENV2 envelope antibody (3H5-1, EMD Millipore) in PBS with 1%
248 bovine serum albumin (BSA). The total number of DENV-positive foci were revealed
249 using a 1:200 horseradish peroxidase-conjugated secondary antibody in PBS plus 1% BSA,
250 and an AEC Peroxidase Substrate kit (Vector Laboratories). This experiment was repeated
251 using cells that were maintained in either glucose or trehalose-containing cell culture media
252 throughout the experiment, and digital images were collected to quantify the total focus-
253 forming units/well and total number of DENV2-positive cells/well. FFU assays were also
254 performed using cell free supernatants isolated from DENV2-infected Aag2 cells that were
255 maintained in either glucose or trehalose-containing cell culture media, examining cell free
256 supernatants at 0, 1, and 3 dpi. Cell free supernatants were stored at -80°C until use and
257 then used to inoculate subconfluent Aag2 cell monolayers that were maintained in glucose-
258 containing cell culture media. FFU assays were also used to quantify the impact of ValA
259 treatment on DENV2 infection. For this experiment, Aag2 cells were inoculated with 40

260 FFU/well DENV2 and co-treated with 0, 0.1, 0.2, and 0.5 mg/mL ValA. Digital images
261 were captured using the Evos XL Core Imaging System.
262
263 **RT-qPCR-based infectivity assays.**
264 Aag2 cells were seeded into 96 well plates and grown to ~70% confluence in either glucose
265 or trehalose-containing cell culture media. Cells were then mock infected or inoculated
266 with 1×10^6 genomic equivalents of DENV2 in either glucose or trehalose-containing cell
267 culture media in triplicate. For the attachment assay, incubation of DENV2 with cells took
268 place at 4°C for 1 hr. and then unbound virus was removed, cells were washed with PBS,
269 and total RNA was extracted and quantified by RT-qPCR. DENV2 viral RNA (vRNA) was
270 normalized by total nanograms of cellular RNA. For the cell entry and replication assay,
271 incubation of DENV2 with cells took place at 25°C for 1 hr. and then unbound virus was
272 removed and replaced with either glucose or trehalose-containing cell culture media. Total
273 RNA was extracted 3 dpi, quantified by RT-qPCR, and normalized using total nanograms
274 of cellular RNA. DENV2 stocks were also generated using Aag2 cells maintained in either
275 glucose or trehalose-containing cell culture media, frozen at -80°C, and then RNA was
276 extracted and quantified using RT-qPCR. FFUs were also measured in these samples,
277 which allowed for determination of the specific infectivity of virions produced from
278 glucose and trehalose-fed cells. Specific infectivity was represented as FFU/vRNA.
279 Amplification of the viral target was performed using a singleplex format in 48-well plates
280 (Illumina) with a total reaction volume of 10 µl. Reverse transcription and quantitative PCR
281 were performed in the same closed tube with 50 ng of total RNA per reaction using the
282 Quantitect RT-qPCR Kit (Qiagen). All primers were used at final concentrations of 4 µM.

283 For amplification of DENV2 vRNA (nt 87–207), Forward: 5′ CAG ATC TCT GAT GAA
284 TAA CCA ACG 3′ and Reverse: 5′ CAT TCC AAG TGA GAA TCT CTT TGT CA 3′
285 DENV2-specific primers were used. The DENV2-specific probe, 5'/56-FAM/CTG CCG
286 ATC/ZEN/TTG CAC ATT ACC ACC GC/3IABkFQ/3′, was used for added specificity.
287 All RT-qPCR reactions were performed using an Eco Illumina and each time point was
288 measured in triplicate. Cycling conditions were 50 °C for 30 min (reverse transcription)
289 and 95 °C for 15 min, followed by 45 cycles of 94 °C for 15 s, 55 °C for 30 s and 72 °C
290 for 30 s. Relative quantities of target cDNA were determined using the Pfaffl method.
291 Student's t tests were performed between groups to determine statistical significance.
292

293 **Results**

294 **Aag2 cells express a secreted trehalase enzyme that can convert trehalose to glucose.**

295 RNA-Seq datasets that characterize gene expression of Aag2 cells reveal high
296 expression of trehalose-6-phosphate synthase (TPS) and trehalase (TREH) homologues
297 (42). Expression of a trehalose 6-phosphate phosphatase (TPP) homologue is low but not
298 absent (Figure 1A). The amino acid sequence of TREH was analyzed using SignalP 6.0
299 and indicated a signal peptide cleavage site between amino acid positions 30 and 31
300 (probability 0.97812) (Figure 1B). PSORT Wolf analysis of the TREH amino acid
301 sequence predicted that it is located in the endoplasmic reticulum, extracellular space,
302 peroxisome, and plasma. Together, these data indicated that Aag2 TREH is a secreted form
303 of the enzyme and exists in the extracellular environment.
304

305 Most cell culture media used to support insect cell growth contains glucose. We
306 reasoned that if Aag2 expressed TREH, and if this enzyme was secreted, it would convert
307 trehalose to glucose and similarly support cell growth. Aag2 cells were grown in both
308 glucose and trehalose-containing cell culture media and passaged at least two times before
309 experiments. Aag2 cells proliferated equally in glucose and trehalose-containing cell
310 culture media (Figure 2A-B). Importantly, over a 3-day time course Aag2 metabolized
311 glucose when maintained on glucose-containing cell culture media, and generated glucose
312 when maintained on trehalose-containing cell culture media (Figure 2C-D).
313

314 ***In vitro* trehalase inhibitor assays show reduction in cell proliferation and reveal**
315 **differences in inhibitor efficacy.**

316 Previous *in vivo* research showed that treatment with trehalase inhibitor ValA at
317 0.2, 0.4, and 1.0 mM led to dose-dependent changes in *Ae. aegypti* development (23). Cell
318 proliferation assays were performed to determine if trehalase inhibitors interfered with
319 Aag2 cell metabolism when maintained in trehalose-containing cell culture media. There
320 was no reduction in cell proliferation when Aag2 cells maintained in glucose-containing
321 cell culture media were treated with 1 mM ValA (Figure 2E). However, when Aag2 cells
322 maintained in trehalose-containing cell culture media were treated with 1 mM ValA, a
323 significant reduction in cell proliferation was evident 3 days post-treatment, which
324 persisted throughout the time course (Figure 2E). To directly test the impact of trehalose
325 analogues on trehalase activity, a dose-dependence assay was performed that quantified
326 conversion of trehalose to glucose. ValA maintained ~75% activity as a trehalase inhibitor
327 at the lowest concentration tested (i.e., 0.008 mM) (Figure 2F). Although 5-ThioTre and 6-

328 $TreNH_2$ maintained ~75% activity at the highest concentration tested (i.e., 1.0 mM), they
329 had no activity at the two lowest concentrations (Figure 2F).
330
331 **RNA-Seq analysis identifies differentially expressed genes involved in trehalose**
332 **metabolism and innate immunity.**
333 Previous research confirmed that key enzymes involved in trehalose metabolism
334 are expressed in Aag2 cells (42). This was somewhat unexpected given that Aag2 cells do
335 not derive from fat body tissue. Very little is known about the response of non-fat body
336 cells and tissues to trehalose. RNA-Seq was performed to characterize the differentially
337 expressed genes in Aag2 cells maintained in glucose and trehalose-containing cell culture
338 media.
339
340 Significant differences in gene expression were observed. There were 157
341 upregulated and 118 downregulated genes in Aag2 cells that were maintained in trehalose-
342 containing cell culture media (Figure 3A). Although TREH expression did not change in
343 the RNA-Seq dataset (Supplementary Table 1) or in a follow-up RT-qPCR validation study
344 (Figure 3B), trehalose transporter 1 Tret1 (AAEL026825) was upregulated 2.7-fold in the
345 presence of trehalose (Supplementary Table 2). Functional annotations of differentially
346 expressed genes also showed significant changes in genes involved in composition of the
347 cell membrane, lipid biosynthesis, sugar conjugation, extracellular matrix, calcium
348 signaling, signal transduction, and mitochondrial function Figure 3C-D). Significant
349 changes in the expression of some innate immunity genes were also noted (Table 1).
350

351 **Passive uptake of a fluorescently labeled trehalose probe.**

352 Considering that Aag2 cells increase expression of Tret1 in response to trehalose
353 while poorly expressing TPP, it is reasonable to expect that these cells can acquire trehalose
354 from the extracellular environment (Supplementary Tables 1-2). To enable testing of
355 whether Aag2 cells can accumulate extracellular trehalose, we synthesized a novel
356 fluorescent trehalose derivative, NBD-Tre, which consists of trehalose conjugated to a
357 fluorescent 2-(7-nitro-2,1,3-benzoxadiazol-4-yl) group (Figure 4A). Aag2 cells that were
358 maintained in trehalose-containing cell culture media were treated with 1.0 mM NBD-Tre
359 probe or a vehicle control for 4 hours, excess probe was removed, cells were washed in
360 cell culture media, and then digital images were taken using a fluorescent microscope. 1.0
361 mM ValA was used to determine if trehalase inhibition would prevent probe degradation
362 and improve cell labeling. Quantifying the mean fluorescent intensity/cell showed a
363 statistically significant increase in signal when cells were treated with the NBD-Tre probe
364 compared to DMSO vehicle control. The addition of trehalase inhibitor ValA did not
365 influence cell labeling (Figure 4B) suggesting that trehalase does not degrade the
366 fluorescent molecule.

367

368 To test if trehalose entered into Aag2 cells using a passive/facilitated process, 0.1
369 mM NBD-Tre probe was suspended in cell culture media with a range of glucose and
370 trehalose concentrations: 0.0, 0.1, 1.0, 10.0, and 25.0 mM. A lower concentration of NBD-
371 Tre probe was used in this experiment because the labeling efficiency of 0.1 mM NBD-Tre
372 in sugar-free cell culture media was equivalent to 1.0 mM NBD-Tre in high glucose or
373 trehalose cell culture media. The mean fluorescent intensity per cell decreased ~10-20% at

374 the highest two concentrations of glucose (Figures 4C,E). In contrast, the mean fluorescent
375 intensity per cell increased at the lowest concentration of trehalose and decreased 40-75%
376 at the three highest concentrations of trehalose (Figures 4D,F). These results support that
377 the trehalose probe entered Aag2 cells through a process of facilitated diffusion, which is
378 consistent with the function of known trehalose transporters such as Tret1 (43).
379

380 **Maintaining Aag2 cells in trehalose-containing cell culture media increases DENV2**
381 **shedding and specific infectivity.**

382 Maintaining Aag2 cells in trehalose-containing cell culture media led to significant
383 changes in gene expression, and trehalose used a facilitated/passive process to accumulate
384 inside of these cells. Transcriptomic changes, which include differential gene expression
385 of key innate immunity genes (Table 1), might influence virus infection. Similarly, an
386 influx of trehalose into intracellular compartments may influence different aspects of the
387 virus life cycle. Dengue virus type 2 (DENV2) was used as a model vector-borne disease
388 to test the hypothesis that trehalose can modify virus infection in insect cells.
389

390 Aag2 cells maintained in glucose-containing cell culture media were inoculated
391 with 20 focus-forming units (FFUs) of DENV2 and the infection was allowed to spread
392 throughout the monolayer for 5 days. Cells were also mock-infected as a negative control.
393 Infected and mock infected cells were then treated with either no glucose cell culture media
394 as a vehicle control or with 1 mM NBD-Tre probe for 4 hours. Aag2 cells were then fixed
395 and stained using an anti-DENV2 3H5.1 Mab and counterstained with Hoescht.
396 Immunofluorescence microscopy revealed diffuse cytoplasmic localization of the NBD-

397 Tre probe and discrete localization of DENV2 envelope (E) protein outside of the nucleus
398 (Figure 5). There was no clear co-localization between these molecules.
399
400 Although the immunofluorescence analysis did not reveal evidence of specific co-
401 localization between trehalose and DENV2 E, the diffuse localization of trehalose Aag2
402 may provide opportunities for interaction with other DENV2 proteins or to influence virus
403 replication. We tested this hypothesis using Aag2 cells maintained in glucose-containing
404 cell culture media, which were inoculated with 20 focus-forming units (FFUs) of DENV2
405 in either glucose or trehalose-containing cell culture media for 1 hour. Unbound virus and
406 cell culture media was removed and replaced with glucose-containing cell culture media.
407 Three days later cell monolayers were fixed and stained with anti-DENV2 MAb and the
408 total number of FFUs per well were quantified. Pre-treatment with either glucose or
409 trehalose-containing cell culture media had no impact on DENV2 infection (Figure 6A).
410 In contrast, when the same experiment was performed using Aag2 cells that were
411 maintained in either glucose or trehalose-containing cell culture media for the duration of
412 the focus forming unit assay, there was a 2-fold increase in FFUs per well in the trehalose-
413 maintained cells (Figures 6B,D). The total number of DENV2 positive cells were
414 quantified in each well, which also revealed a 2-fold increase in the trehalose-maintained
415 cells (Figures 6C,D).
416
417 To determine the stage of the virus life cycle that was affected by trehalose, an
418 attachment assay was performed using Aag2 cells that were maintained in either glucose
419 or trehalose-containing cell culture media. Cells were inoculated with 20 FFUs DENV2 in

420 glucose-containing cell culture media at 4 °C for 1 hour, unbound virus was removed, cells
421 were washed with cell culture media, and total RNA was extracted from cell monolayers.
422 RT-qPCR analysis showed no difference in the attachment of DENV2 to Aag2 cells
423 maintained in either glucose or trehalose-containing cell culture media (Figure 6E). A cell
424 entry assay was then performed, which allowed DENV2 to attach and enter Aag2 cells at
425 37 °C for 4 hours. RT-qPCR analysis showed a statistically significant increase in cell entry
426 of DENV2 inside of Aag2 cells that were maintained in trehalose-containing cell culture
427 media (Figure 6F). Supernatants were then collected from DENV2-infected Aag2 cells that
428 were maintained in either glucose or trehalose-containing cell culture media and stored as
429 viral stocks. Viral stocks were tested to determine the total FFUs/well in a 5 µL inoculum
430 onto Aag2 cells that were maintained in glucose-containing cell culture media. Consistent
431 with previous experiments, significantly more DENV2 was shed from Aag2 cells that were
432 maintained in trehalose-containing cell culture media by day 3 post-infection (dpi) (Figure
433 6G). To test the quality of virions produced by Aag2 cells maintained in either glucose or
434 trehalose-containing cell culture media, virus stocks were prepared from each condition at
435 5 dpi, and then FFU and RT-qPCR assays were performed. The total FFUs per mL were
436 normalized by vRNA (FFU/vRNA) to determine specific infectivity of virus stocks. The
437 specific infectivity of DENV2 produced from Aag2 cells maintained in trehalose-
438 containing cell culture media was 2-fold greater (Figure 6H).
439

440 **Trehalose promotes accumulation of intracellular lipids.**

441 Previous research suggests that trehalose induces autophagy in mammalian cells,
442 although autophagy's role in virus infection is varied (32-36, 39, 44). The consensus is that

443 DENV benefits from autophagy in mammalian cells by enhancing cell survival and
444 promoting virus maturation (45-49). The role of autophagy in arbovirus infection in insect
445 cells is less clear, and conventional autophagy inducers and inhibitors may respond
446 differently in insect cells (44, 50). Trehalose can also be converted to glucose and used as
447 a substrate for lipogenesis (42).
448
449 RNA-Seq analysis revealed significant changes in gene expression related to
450 integral/intrinsic membrane components, and the main function of autophagy is to
451 accumulate and utilize lipids to enhance cell survival. We used Nile Red staining to
452 determine if trehalose modified the lipid environment of Aag2 cells. We identified a slight,
453 yet significant increase in intracellular lipid accumulation in Aag2 cells that were
454 maintained in trehalose-containing cell culture media (Figure 7A-B).
455
456 **DENV2 infection does not impact trehalose metabolism.**
457 Previous research has shown that DENV manipulates the metabolism of its host
458 cell to promote replication. Different parameters of trehalose metabolism were tested
459 during DENV2 infection to determine if this pathway is manipulated in Aag2 cells. Aag2
460 cells maintained in trehalose-containing cell culture media were either mock infected or
461 infected with DENV2 and conversion of trehalose to glucose was assessed on 1, 3, 5, and
462 7 dpi. DENV2 infection did not influence trehalase activity (Figure 8A). The impact of
463 DENV2 infection on trehalose uptake was also tested by infecting Aag2 cells that were
464 maintained in glucose-containing cell culture media with 0, 1, 10, 100, and 500 FFUs and
465 then labeling cells with 0.1 mM NBD-Tre 3 dpi. There was no difference in mean

466 fluorescence intensity per cell, therefore DENV2 infection did not influence trehalose
467 uptake (Figure 8B).
468
469 **Trehalase inhibition reduces cell viability and DENV infection in trehalose-dependent**
470 **Aag2 cells.**
471 We previously showed that trehalase inhibition reduced cell proliferation when
472 cells were maintained in trehalose-containing cell culture media (Figure 2E). We
473 hypothesized that this activity would reduce DENV productivity. As expected, ValA
474 treatment did not reduce cell viability or DENV productivity in Aag2 cells that were
475 maintained in glucose-containing cell culture media, and surprisingly increased DENV
476 productivity by 50% (Figure 9A-C). In contrast, ValA treatment significantly reduced cell
477 viability and DENV productivity in Aag2 cells that were maintained in trehalose-
478 containing cell culture media (Figure 9D-F). It is important to note that a FFU assay was
479 not performed directly on Aag2 cells that were maintained on trehalose-containing cell
480 culture media because the addition of ValA prevents establishment of a monolayer, which
481 is required for the assay. Instead, cell-free supernatants were harvested from ValA-treated
482 cells and used for downstream FFU assays performed on Aag2 cells that were maintained
483 on glucose-containing cell culture media.
484
485 **Discussion**
486 Control of *Aedes* spp. disease vectors is an important area of ongoing research due
487 to concerns regarding vaccine limitations, pesticide resistance, and increased geographic
488 spread (6). Trehalase inhibitors have been previously characterized as a novel class of

489 putative insecticides, potentially effective for controlling *Aedes* spp. disease vectors due to
490 the vital importance of trehalose as a blood sugar during mosquito development (14, 15,
491 17, 18, 20, 24, 25, 30, 40). Our previous research has revealed that the commercially
492 available trehalase inhibitor ValA negatively impacts mosquito development *in vivo* when
493 applied directly to the larval environment by showing dose-dependent activity delaying
494 egg hatch, pupation, eclosure, and flight of adult *Ae. Aegypti* mosquitoes (23).
495
496 Here, we describe the use of an *in vitro* model to screen for trehalase inhibitors in
497 *Ae. aegypti* and determine the impact of trehalose metabolism on a mosquito-borne virus.
498 ValA and novel trehalase inhibitors (5-ThioTre, 6-TreNH_2) prevented conversion of cell
499 culture media trehalose to glucose. ValA had the strongest activity, which significantly
500 reduced cell proliferation. Differences in the activity of trehalose analogues seen *in vitro*
501 and *in vivo* suggest that there are opportunities to optimize trehalase inhibitors for target
502 species (23). Our *in vitro* assay is a platform that could be used for high throughput studies
503 to develop targeted trehalose analogues.
504
505 RNA-Seq analysis showed that Tret1 expression was induced in cells that were
506 maintained in trehalose-containing cell culture media. The Aag2 cell line was originally
507 generated from whole homogenized embryos. Cells within the culture exhibit differing
508 morphologies, and it has been suggested that the varying morphologies of mosquito cells
509 in culture may be indicative of the presence of a diversity of embryonic and differentiated
510 cell types (51). Aag2 cells were not derived from fat body cells or tissue, which is where
511 Tret1 is concentrated *in vivo* (43). The role of Tret1 in peripheral cells and tissues is

512 unknown. Considering that the machinery for trehalose synthesis was lacking in Aag2
513 cells, we hypothesized that these cells may use Tret1 for trehalose uptake rather than
514 excretion. Previous research has shown that Tret1 is a facilitated/passive transporter (43).
515 We confirmed that Aag2 cells could accumulate a novel fluorescent trehalose probe, NBD-
516 Tre, and that uptake was prevented if unlabeled trehalose was present. This supports
517 facilitated/passive uptake of trehalose in Aag2 cells.
518
519 Entry of trehalose into Aag2 cells may have led to differential gene expression as
520 noted in the RNA-Seq dataset, although the presence of trehalose also induced expression
521 of integrin proteins, which mediate signaling from the cell surface. Significant differences
522 in gene expression were present in genes involved in composition of the cell membrane,
523 lipid biosynthesis, sugar conjugation, extracellular matrix, calcium signaling, signal
524 transduction, and mitochondrial function. These global changes in gene expression may
525 explain why the physiological role of trehalose extends beyond a simple source of fuel.
526 Trehalase inhibition can impact a wide array of physiological functions in insects including
527 chitin synthesis, stress protection, larval and pupal development (14, 17-20, 24-26, 28).
528
529 Considering that trehalose enters Aag2 cells and leads to significant changes in
530 gene expression, we hypothesized that the environment of a trehalose-fed insect cell was
531 different enough to influence virus infection. This was supported by previous data
532 suggesting that trehalose can induce autophagy and that DENV2 benefits from autophagy
533 by prolonging cell survival and enhancing virus maturation (45-49). We found that Aag2
534 cells that were maintained in trehalose-containing cell culture media promoted DENV2

535 cell entry, which led to a higher number of infected cells, and increased virus shedding. In
536 mammalian cells, trehalose is an inducer of autophagy and can block autophagic flux from
537 autophagosomes to autolysosomes (39). DENV2 also induces the autophagy pathway, and
538 infection is reduced when autophagy is inhibited (45-49). It is possible that trehalose
539 increases DENV2 infection in Aag2 cells by promoting autophagy and enhancing virus
540 cell entry through modification of cell membranes. Previous research suggests that the
541 relationship between autophagy and DENV infection in Aag2 cells is complicated and that
542 conventional autophagy inhibitors may not work as expected in these cells (44). Instead,
543 we used Nile Red staining as a proxy to quantify changes to the intracellular lipid
544 environment. Nile Red staining revealed an increase in intracellular lipids in Aag2 cells
545 maintained on trehalose-containing cell culture media. It is important to note that trehalose
546 is the main blood sugar in insects, and it may not have the same influence on autophagy as
547 seen in mammalian cells.
548
549 Trehalose can also be converted to glucose, which is a substrate for lipogenesis. It
550 is possible that trehalose stimulates lipogenesis and the production of triglycerides and
551 associated fatty acids that promote virus replication and synthesis of more infectious viral
552 particles. RNA-Seq analysis showed that trehalose-fed cells had a 55% downregulation of
553 phosphoenolpyruvate carboxykinase (i.e., AAEL000006) and a 20% upregulation of fatty
554 acid synthase (i.e., AAEL001194) (Supplementary Table 1). Further, one of the most
555 upregulated genes (714%) was elongation of very long chain fatty acids protein 4
556 (AAEL004947). Together, these changes in gene expression may have been responsible

557 for the increase in intracellular lipids and perhaps the increase in virus replication and
558 shedding.
559
560 The specific infectivity of DENV2 also increased when virus stocks were produced
561 from Aag2 cells that were maintained in trehalose-containing cell culture media. The
562 mechanism of action that led to increased specific infectivity is unknown, although
563 trehalose is widely known for its ability to prevent heat and cold shock and it is used as a
564 cryoprotectant (52-58). Trehalose may provide some membrane or protein stabilizing
565 activity that either allows virus production and shedding to occur more efficiently or it
566 simply allows more virus to survive a freeze-thaw event. Autophagy has also been linked
567 to DENV maturation, which suggests that trehalose may facilitate production of more
568 mature virions (49). It is important to note that the trehalose concentration used in our cell
569 culture media is 20-50-fold less than what is typically used for cryoprotection (52-54, 59-
570 61).
571
572 Trehalase inhibition interferes with multiple physiological pathways in insects, and
573 we found that ValA reduced cell proliferation in Aag2 cells that were maintained in
574 trehalose-containing cell culture media. It was reasonable to hypothesize that trehalase
575 inhibition would also reduce DENV productivity. We showed that 1.0 mM ValA causes a
576 90% reduction in cell viability 5 days post-treatment in Aag2 cells that were maintained in
577 trehalose-containing cell culture media. The reduction in cell viability correlated with an
578 approximately 75% decrease in DENV vRNA shedding. *In vivo* studies show deficits in
579 *Ae. aegypti* egg hatch rate, larval development, pupation, and eclosure (23). Considering

580 that vertical transmission is less important for the maintenance and transmission of DENV
581 in a natural environment, trehalase inhihibition in larval habitats would likely not impact
582 DENV in a meaningful way. It is unclear how trehalase inhibition impacts adult *Ae. aegypti*
583 at this time, although these data suggest that targeting adults could simultaneously reduce
584 mosquito and virus fitness.
585
586 This manuscript describes an *in vitro* model that can be used to rapidly screen novel
587 trehalase inhibitors and probes and underscores the importance of trehalose metabolism in
588 *Ae. aegypti* physiology and the transmission of a mosquito-borne virus. These data
589 facilitate the future development of targeted trehalase analogues that will reduce
590 populations of disease vectors and related viruses with minimal off-target effects.
591

592 **Acknowledgements**
593 This work was supported through start-up funds from Central Michigan University College
594 of Medicine. BMS was supported by a grant from the National Institutes of Health
595 (R15AI117670).
596

597 **Figure legends**
598

599 **Figure 1. Trehalose metabolism genes expressed in Aag2 cells.** (A) Trehalose pathway
600 showing *Ae. aegypti* enzymes involved in synthesis: TPS; AAEL006446 and TPP;
601 AAEL010684 and catabolism: TREH; AAEL009658. (B) SignalP 6.0 prediction of a
602 signal peptide in TREH; AAEL009658.

603

604 **Figure 2. Trehalose supports the growth of Aag2 cells.** (A) Representative image of
605 Aag2 cells at 20X magnification maintained in either glucose (GLU) or trehalose (TRE)-
606 containing cell culture media. (B) Cell proliferation assay of Aag2 cells maintained in
607 either glucose (circles) or trehalose (squares)-containing cell culture media was performed
608 for 7 days (D0-D7). (C) Glucose assay of Aag2 cell supernatant at days 0, 1, 2, and 3 post-
609 feeding (D0-D3) with glucose-containing cell culture media. (D) Glucose assay of Aag2
610 cell supernatant at days 0, 1, 2, and 3 (D0-D3) post-feeding with trehalose-containing cell
611 culture media. (E) Cell proliferation assay of Aag2 cells grown in either glucose-containing
612 cell culture media with (square) or without (circle) 1.0 mM ValA or trehalose-containing
613 cell culture media with (upside down triangle) or without (triangle) 1.0 mM ValA. (F)
614 Glucose assay of Aag2 cell supernatants from cells maintained in trehalose-containing cell
615 culture media and treated with 0.008-1 mM ValA, 5-ThioTre, and 6-TreNH2. Assays were
616 performed in triplicate. Unpaired Student's t tests were performed between groups to assess
617 statistical significance. Standard deviations are shown.

618

619 **Figure 3. RNA-Seq analysis and differentially expressed genes.** (A) Volcano plot of
620 upregulated (157) and downregulated (118) differentially expressed genes present in Aag2
621 cells that were maintained in trehalose-containing cell culture media. (B) RT-qPCR
622 analysis of TREH expression in Aag2 cells that were maintained in either glucose (G) or
623 trehalose (T)-containing cell culture media on 0-3 dpt (D0-D3). (C) Functional annotation
624 categories present in upregulated genes. (D) Functional annotation categories in
625 downregulated genes.

626

627 **Figure 4. NBD-Tre probe uptake in Aag2 cells.** (A) Chemical structure of fluorescently
628 labeled trehalose probe NBD-Tre. (B) Aag2 cells were treated with either vehicle control
629 (DMSO), 1.0 mM NBD-Tre probe, or with 1.0 mM NBD-Tre probe and 1.0 mM ValA in
630 glucose free cell culture media for 4 hours and then mean fluorescence intensity/cell was
631 determined. (C-D) Aag2 cells were treated with 1.0 mM NBD-Tre probe in the presence
632 of (C) 0, 0.1, 1, 10, and 25 mM glucose and (D) 0, 0.1, 1, 10, and 25 mM trehalose for 4
633 hours and then mean fluorescence intensity/cell was determined. (E-F) Representative
634 images of Aag2 cells that were treated with 1.0 mM NBD-Tre probe in the presence of (E)
635 0, 0.1, 1, 10, and 25 mM glucose and (F) 0, 0.1, 1, 10, and 25 mM trehalose with a Hoescht
636 nuclear counterstain. Assays were performed in triplicate. Unpaired Student's t tests were
637 performed between groups to assess statistical significance. Standard deviations are shown.

638

639 **Figure 5. Co-localization of NBD-Tre and DENV2 in Aag2 cells.** Aag2 cells were
640 uninfected (Mock) or infected with DENV2 for 5 days and then treated with no glucose
641 cell culture media alone (Vehicle) or 1 mM NBD-Tre probe for 4 hours. Aag2 cells were
642 then fixed and stained with anti-DENV2 Mab and digital images were obtained at 20X
643 magnification. Hoescht nuclear stain was added to each condition.

644

645 **Figure 6. Trehalose promotes DENV2 cell entry and virus shedding.** Aag2 cells were
646 Mock infected or infected with DENV in either glucose (GLU) or trehalose (TRE)-
647 containing cell culture media. (A) Trehalose-containing cell culture media was only present
648 during inoculation and was then exchanged for glucose-containing cell culture media and

649 focus-forming units were quantified 3 dpi. (B) Trehalose-containing cell culture media was
650 present during inoculation and for the three days prior to a focus-forming unit assay. (C)
651 The total number of DENV2 positive cells per well were quantified from (B). (D)
652 Representative images from (B) showing distinct foci are shown. (E) An attachment assay
653 was performed by incubating DENV2 with Aag2 cells at 4°C for 1 hour. Unbound virus
654 was removed, cells were washed with PBS, and total RNA was extracted and quantified by
655 RT-qPCR. DENV2 viral RNA (vRNA) was normalized by total nanograms of cellular
656 RNA (F) A cell entry/replication assay was performed by incubating DENV2 with Aag2
657 cells at 25°C for 1 hour. Unbound virus was removed and replaced with either glucose or
658 trehalose-containing cell culture media. Total RNA was extracted 3 dpi, quantified by RT-
659 qPCR, an DENV2 vRNA was normalized using total nanograms of cellular RNA. (G) A
660 virus shedding assay was performed by collecting cell free supernatants at 0, 1, and 3 dpi
661 from Aag2 cells that were inoculated with DENV2 in either glucose or trehalose-containing
662 cell culture media. Cell free supernatants were used to inoculate monolayers of Aag2 cells
663 grown in glucose-containing cell culture media and focus forming unit assays were used to
664 quantify the infectious units present in each sample. (H) DENV2 stocks were generated
665 from Aag2 cells that were grown in either glucose or trehalose-containing cell culture
666 media. Focus forming unit assays were performed to quantify the infectivity of each stock.
667 Total RNA was also extracted from virus stocks and DENV2 vRNA was quantified using
668 RT-qPCR. Specific infectivity was derived by normalizing the total number of focus
669 forming units in a sample by its vRNA content (i.e., FFU/vRNA). Assays were performed
670 in triplicate. Unpaired Student's t tests were performed between groups to assess statistical
671 significance. Standard deviations are shown.

672

673 **Figure 7. Trehalose promotes intracellular lipid accumulation in Aag2 cells.** (A)
674 Intracellular lipids were labeled in Aag2 cells maintained in either glucose (GLU) or
675 trehalose (TRE) cell culture media using either vehicle control (DMSO) or Nile Red. Cells
676 were fixed and digital images were obtained at 20X magnification. Hoescht nuclear stain
677 was added to each condition. (B) The corrected total cell fluorescence (CTCF) was
678 quantified using the integrated density of 60 individual cells per condition. Assays were
679 performed in triplicate. Unpaired Student's t tests were performed between groups to assess
680 statistical significance. Standard deviations are shown.

681

682 **Figure 8. DENV2 infection does not influence trehalase activity or trehalose uptake.**
683 (A) A glucose assay was performed on cell-free supernatants taken from Aag2 cells
684 maintained in trehalose-containing cell culture media that were either uninfected (Mock)
685 or infected with DENV2 for 1, 3, 5, and 7 dpi. (B) A trehalose probe uptake assay was
686 performed on Aag2 cells that were either uninfected (Mock) or infected with 1, 10, 100,
687 and 500 FFUs of DENV2 5 dpi. 1.0 mM NBD-Tre probe was added to cells in glucose free
688 cell culture media for 4 hours. Unbound probe was removed, and then digital images were
689 obtained at 20X magnification. Mean fluorescence intensity was determined for 50
690 individual cells per condition. Assays were performed in triplicate. Unpaired Student's t
691 tests were performed between groups to assess statistical significance. Standard deviations
692 are shown.

693

694 **Figure 9. Validamycin A reduces cell viability and DENV2 productivity when Aag2**
695 **cells are maintained in trehalose-containing cell culture media.** (A) Subconfluent Aag2
696 cells maintained in glucose-containing cell culture media were treated with 0, 0.2, 0.4, and
697 1.0 mM ValA for 5 days and then trypan blue exclusion assays were performed to quantify
698 percent cell viability. (B) Subconfluent Aag2 cells maintained in glucose-containing cell
699 culture media were inoculated with 20 FFUs of DENV for 1 hour, followed by treatment
700 with 0, 0.2, 0.4, and 1.0 mM ValA for 5 days. vRNA was extracted from equivalent
701 volumes of cell free supernatants and quantified by RT-qPCR. (C) Subconfluent Aag2 cells
702 maintained in glucose-containing cell culture media were inoculated with 20 FFUs of
703 DENV for 1 hour, followed by treatment with 0, 0.2, 0.4, and 1.0 mM ValA for 3 days.
704 FFU assays were performed to quantify the total FFUs present in each well. (D)
705 Subconfluent Aag2 cells maintained in trehalose-containing cell culture media were treated
706 with 0, 0.2, 0.4, and 1.0 mM ValA for 5 days and then trypan blue exclusion assays were
707 performed to quantify percent cell viability. (E) Subconfluent Aag2 cells maintained in
708 trehalose-containing cell culture media were inoculated with 20 FFUs of DENV for 1 hour,
709 followed by treatment with 0, 0.2, 0.4, and 1.0 mM ValA for 5 days. vRNA was extracted
710 from equivalent volumes of cell free supernatants and quantified by RT-qPCR. (F)
711 Subconfluent Aag2 cells maintained in trehalose-containing cell culture media were
712 inoculated with 20 FFUs of DENV for 1 hour, followed by treatment with 0, 0.2, 0.4, and
713 1.0 mM ValA for 3 days. Cell free supernatants were harvested and used for a downstream
714 FFU assay performed on Aag2 cells maintained on glucose-containing cell culture media,
715 which quantified the total FFUs present in each well. Assays were performed in triplicate.

716 Unpaired Student's t tests were performed between groups to assess statistical significance.
717 Standard deviations are shown.
718
719 **Supplementary Table 1. Complete readcount and FPKM list of all genes in GLU vs**
720 **TRE Aag2 cells.**
721
722 **Supplementary Table 2. Complete readcount and FPKM list of upregulated genes in**
723 **GLU vs TRE Aag2 cells.**
724
725 **Supplementary Table 3. Complete readcount and FPKM list of all downregulated in**
726 **GLU vs TRE Aag2 cells.**
727
728 **References**

729 1. Paul LM, Carlin ER, Jenkins MM, Tan AL, Barcellona CM, Nicholson CO, et al.
730 Dengue virus antibodies enhance Zika virus infection. Clin Transl Immunology.
731 2016;5(12):e117.
732 2. Masel J, McCracken MK, Gleeson T, Morrison B, Rutherford G, Imrie A, et al.
733 Does prior dengue virus exposure worsen clinical outcomes of Zika virus infection? A
734 systematic review, pooled analysis and lessons learned. PLoS Negl Trop Dis.
735 2019;13(1):e0007060.
736 3. Guzman MG, Alvarez M, Halstead SB. Secondary infection as a risk factor for
737 dengue hemorrhagic fever/dengue shock syndrome: an historical perspective and role of
738 antibody-dependent enhancement of infection. Arch Virol. 2013;158(7):1445-59.
739 4. Obi JO, Gutiérrez-Barbosa H, Chua JV, Deredge DJ. Current Trends and
740 Limitations in Dengue Antiviral Research. Trop Med Infect Dis. 2021;6(4).
741 5. Dighe SN, Ekwudu O, Dua K, Chellappan DK, Katavic PL, Collet TA. Recent
742 update on anti-dengue drug discovery. Eur J Med Chem. 2019;176:431-55.
743 6. Conway MJ, Haslitt DP, Swarts BM. Targeting Aedes aegypti Metabolism with
744 Next-Generation Insecticides. Viruses. 2023;15(2).
745 7. Rose RI. Pesticides and public health: integrated methods of mosquito
746 management. Emerg Infect Dis. 2001;7(1):17-23.

747 8. Moyes CL, Vontas J, Martins AJ, Ng LC, Koou SY, Dusfour I, et al. Contemporary
748 status of insecticide resistance in the major Aedes vectors of arboviruses infecting humans.
749 PLoS Negl Trop Dis. 2017;11(7):e0005625.
750 9. Zulfa R, Lo WC, Cheng PC, Martini M, Chuang TW. Updating the Insecticide
751 Resistance Status of Aedes aegypti and Aedes albopictus in Asia: A Systematic Review
752 and Meta-Analysis. Trop Med Infect Dis. 2022;7(10).
753 10. Roberts DR, Andre RG. Insecticide resistance issues in vector-borne disease
754 control. Am J Trop Med Hyg. 1994;50(6 Suppl):21-34.
755 11. Kasai S, Itokawa K, Uemura N, Takaoka A, Furutani S, Maekawa Y, et al.
756 Discovery of super-insecticide-resistant dengue mosquitoes in Asia: Threats of
757 concomitant knockdown resistance mutations. Sci Adv. 2022;8(51):eabq7345.
758 12. Du Y, Nomura Y, Zhorov BS, Dong K. Sodium Channel Mutations and Pyrethroid
759 Resistance in Aedes aegypti. Insects. 2016;7(4).
760 13. Amelia-Yap ZH, Chen CD, Sofian-Azirun M, Low VL. Pyrethroid resistance in the
761 dengue vector Aedes aegypti in Southeast Asia: present situation and prospects for
762 management. Parasit Vectors. 2018;11(1):332.
763 14. Zhang L, Qiu LY, Yang HL, Wang HJ, Zhou M, Wang SG, et al. Study on the
764 Effect of Wing Bud Chitin Metabolism and Its Developmental Network Genes in the
765 Brown Planthopper, Nilaparvata lugens, by Knockdown of TRE Gene. Front Physiol.
766 2017;8:750.
767 15. Xia Y, Clarkson JM, Charnley AK. Trehalose-hydrolysing enzymes of
768 Metarhizium anisopliae and their role in pathogenesis of the tobacco hornworm, Manduca
769 sexta. J Invertebr Pathol. 2002;80(3):139-47.
770 16. Wyatt GR, Kale GF. The chemistry of insect hemolymph. II. Trehalose and other
771 carbohydrates. J Gen Physiol. 1957;40(6):833-47.
772 17. Wegener G, Macho C, Schloder P, Kamp G, Ando O. Long-term effects of the
773 trehalase inhibitor trehazolin on trehalase activity in locust flight muscle. J Exp Biol.
774 2010;213(Pt 22):3852-7.
775 18. Wegener G, Tschiedel V, Schloder P, Ando O. The toxic and lethal effects of the
776 trehalase inhibitor trehazolin in locusts are caused by hypoglycaemia. J Exp Biol.
777 2003;206(Pt 7):1233-40.
778 19. Thorat LJ, Gaikwad SM, Nath BB. Trehalose as an indicator of desiccation stress
779 in Drosophila melanogaster larvae: a potential marker of anhydrobiosis. Biochem Biophys
780 Res Commun. 2012;419(4):638-42.
781 20. Tatun N, Wangsantitham O, Tungjitwitayakul J, Sakurai S. Trehalase activity in
782 fungus-growing termite, Odontotermes feae (Isoptera: Termitideae) and inhibitory effect
783 of validamycin. J Econ Entomol. 2014;107(3):1224-32.
784 21. Tang B, Yang M, Shen Q, Xu Y, Wang H, Wang S. Suppressing the activity of
785 trehalase with validamycin disrupts the trehalose and chitin biosynthesis pathways in the
786 rice brown planthopper, Nilaparvata lugens. Pestic Biochem Physiol. 2017;137:81-90.
787 22. Shukla E, Thorat LJ, Nath BB, Gaikwad SM. Insect trehalase: physiological
788 significance and potential applications. Glycobiology. 2015;25(4):357-67.
789 23. Marten AD, Stothard AI, Kalera K, Swarts BM, Conway MJ. Validamycin A
790 Delays Development and Prevents Flight in Aedes aegypti (Diptera: Culicidae). J Med
791 Entomol. 2020;57(4):1096-103.

792 24. Katagiri N, Ando O, Yamashita O. Reduction of glycogen in eggs of the silkworm,
793 Bombyx mori, by use of a trehalase inhibitor, trehazolin, and diapause induction in
794 glycogen-reduced eggs. J Insect Physiol. 1998;44(12):1205-12.
795 25. Liebl M, Nelius V, Kamp G, Ando O, Wegener G. Fate and effects of the trehalase
796 inhibitor trehazolin in the migratory locust (Locusta migratoria). J Insect Physiol.
797 2010;56(6):567-74.
798 26. Chen J, Zhang D, Yao Q, Zhang J, Dong X, Tian H, et al. Feeding-based RNA
799 interference of a trehalose phosphate synthase gene in the brown planthopper, Nilaparvata
800 lugens. Insect Mol Biol. 2010;19(6):777-86.
801 27. Chen J, Tang B, Chen H, Yao Q, Huang X, Zhang D, et al. Different functions of
802 the insect soluble and membrane-bound trehalase genes in chitin biosynthesis revealed by
803 RNA interference. PLoS One. 2010;5(4):e10133.
804 28. Asano N, Yamaguchi T, Kameda Y, Matsui K. Effect of validamycins on
805 glycohydrolases of Rhizoctonia solani. J Antibiot (Tokyo). 1987;40(4):526-32.
806 29. Murphy TA, Wyatt GR. ENZYMATIC REGULATION OF TREHALOSE AND
807 GLYCOGEN SYNTHESIS IN THE FAT BODY OF AN INSECT. Nature.
808 1964;202:1112-3.
809 30. Becker A, Schloder P, Steele JE, Wegener G. The regulation of trehalose
810 metabolism in insects. Experientia. 1996;52(5):433-9.
811 31. Arguelles JC. Why can't vertebrates synthesize trehalose? J Mol Evol. 2014;79(3-
812 4):111-6.
813 32. Yuan S, Zhang ZW, Li ZL. Trehalose May Decrease the Transmission of Zika
814 Virus to the Fetus by Activating Degradative Autophagy. Front Cell Infect Microbiol.
815 2017;7:402.
816 33. Wu Q, Jiang D, Huang C, van Dyk LF, Li L, Chu HW. Trehalose-mediated
817 autophagy impairs the anti-viral function of human primary airway epithelial cells. PLoS
818 One. 2015;10(4):e0124524.
819 34. Clark AE, Zhu Z, Krach F, Rich JN, Yeo GW, Spector DH. Zika virus is transmitted
820 in neural progenitor cells via cell-to-cell spread and infection is inhibited by the autophagy
821 inducer trehalose. J Virol. 2021;95(5).
822 35. Clark AE, Sabalza M, Gordts P, Spector DH. Human Cytomegalovirus Replication
823 Is Inhibited by the Autophagy-Inducing Compounds Trehalose and SMER28 through
824 Distinctively Different Mechanisms. J Virol. 2018;92(6).
825 36. Belzile JP, Sabalza M, Craig M, Clark AE, Morello CS, Spector DH. Trehalose, an
826 mTOR-Independent Inducer of Autophagy, Inhibits Human Cytomegalovirus Infection in
827 Multiple Cell Types. J Virol. 2016;90(3):1259-77.
828 37. Rodríguez-Navarro JA, Rodríguez L, Casarejos MJ, Solano RM, Gómez A,
829 Perucho J, et al. Trehalose ameliorates dopaminergic and tau pathology in parkin
830 deleted/tau overexpressing mice through autophagy activation. Neurobiol Dis.
831 2010;39(3):423-38.
832 38. Perucho J, Casarejos MJ, Gomez A, Solano RM, de Yébenes JG, Mena MA.
833 Trehalose protects from aggravation of amyloid pathology induced by isoflurane
834 anesthesia in APP(swe) mutant mice. Curr Alzheimer Res. 2012;9(3):334-43.
835 39. Zhang X, Chen S, Song L, Tang Y, Shen Y, Jia L, et al. MTOR-independent,
836 autophagic enhancer trehalose prolongs motor neuron survival and ameliorates the

autophagic flux defect in a mouse model of amyotrophic lateral sclerosis. Autophagy. 2014;10(4):588-602.
40. Danielson ND, Collins J, Stothard AI, Dong QQ, Kalera K, Woodruff PJ, et al. Degradation-resistant trehalose analogues block utilization of trehalose by hypervirulent Clostridioides difficile. Chem Commun (Camb). 2019;55(34):5009-12.
41. Kalera K, Liu R, Lim J, Pathirage R, Swanson DH, Johnson UG, et al. Targeting Mycobacterium tuberculosis Persistence through Inhibition of the Trehalose Catalytic Shift. ACS Infect Dis. 2024;10(4):1391-404.
42. Marten AD, Tift CT, Tree MO, Bakke J, Conway MJ. Chronic depletion of vertebrate lipids in A*edes aegypti* cells dysregulates lipid metabolism and inhibits innate immunity without altering dengue infectivity. In Press ed. PLoS Neglected Tropical Diseases2022.
43. Kikawada T, Saito A, Kanamori Y, Nakahara Y, Iwata K, Tanaka D, et al. Trehalose transporter 1, a facilitated and high-capacity trehalose transporter, allows exogenous trehalose uptake into cells. Proc Natl Acad Sci U S A. 2007;104(28):11585-90.
44. Brackney DE, Correa MA, Cozens DW. The impact of autophagy on arbovirus infection of mosquito cells. PLoS Negl Trop Dis. 2020;14(5):e0007754.
45. Heaton NS, Perera R, Berger KL, Khadka S, Lacount DJ, Kuhn RJ, et al. Dengue virus nonstructural protein 3 redistributes fatty acid synthase to sites of viral replication and increases cellular fatty acid synthesis. Proc Natl Acad Sci U S A. 2010;107(40):17345-50.
46. Lee YR, Lei HY, Liu MT, Wang JR, Chen SH, Jiang-Shieh YF, et al. Autophagic machinery activated by dengue virus enhances virus replication. Virology. 2008;374(2):240-8.
47. Heaton NS, Randall G. Dengue virus-induced autophagy regulates lipid metabolism. Cell Host Microbe. 2010;8(5):422-32.
48. McLean JE, Wudzinska A, Datan E, Quaglino D, Zakeri Z. Flavivirus NS4A-induced autophagy protects cells against death and enhances virus replication. J Biol Chem. 2011;286(25):22147-59.
49. Mateo R, Nagamine CM, Spagnolo J, Méndez E, Rahe M, Gale M, Jr., et al. Inhibition of cellular autophagy deranges dengue virion maturation. J Virol. 2013;87(3):1312-21.
50. Chen TY, Smartt CT. Activation of the autophagy pathway decreases dengue virus infection in Aedes aegypti cells. Parasit Vectors. 2021;14(1):551.
51. Fredericks AC, Russell TA, Wallace LE, Davidson AD, Fernandez-Sesma A, Maringer K. Aedes aegypti (Aag2)-derived clonal mosquito cell lines reveal the effects of pre-existing persistent infection with the insect-specific bunyavirus Phasi Charoen-like virus on arbovirus replication. PLoS Negl Trop Dis. 2019;13(11):e0007346.
52. Yoshida K, Ono F, Chouno T, Perocho BR, Ikegami Y, Shirakigawa N, et al. Cryoprotective enhancing effect of very low concentration of trehalose on the functions of primary rat hepatocytes. Regen Ther. 2020;15:173-9.
53. Erdag G, Eroglu A, Morgan J, Toner M. Cryopreservation of fetal skin is improved by extracellular trehalose. Cryobiology. 2002;44(3):218-28.
54. Beattie GM, Crowe JH, Lopez AD, Cirulli V, Ricordi C, Hayek A. Trehalose: a cryoprotectant that enhances recovery and preserves function of human pancreatic islets after long-term storage. Diabetes. 1997;46(3):519-23.

883 55. Elbein AD, Pan YT, Pastuszak I, Carroll D. New insights on trehalose: a
884 multifunctional molecule. Glycobiology. 2003;13(4):17R-27R.
885 56. Liu K, Dong Y, Huang Y, Rasgon JL, Agre P. Impact of trehalose transporter
886 knockdown on Anopheles gambiae stress adaptation and susceptibility to Plasmodium
887 falciparum infection. Proc Natl Acad Sci U S A. 2013;110(43):17504-9.
888 57. Breeuwer P, Lardeau A, Peterz M, Joosten HM. Desiccation and heat tolerance of
889 Enterobacter sakazakii. J Appl Microbiol. 2003;95(5):967-73.
890 58. Versele M, Thevelein JM. Lre1 affects chitinase expression, trehalose
891 accumulation and heat resistance through inhibition of the Cbk1 protein kinase in
892 Saccharomyces cerevisiae. Mol Microbiol. 2001;41(6):1311-26.
893 59. Hu Y, Liu X, Liu F, Xie J, Zhu Q, Tan S. Trehalose in Biomedical
894 Cryopreservation-Properties, Mechanisms, Delivery Methods, Applications, Benefits, and
895 Problems. ACS Biomater Sci Eng. 2023;9(3):1190-204.
896 60. Solocinski J, Osgood Q, Wang M, Connolly A, Menze MA, Chakraborty N. Effect
897 of trehalose as an additive to dimethyl sulfoxide solutions on ice formation, cellular
898 viability, and metabolism. Cryobiology. 2017;75:134-43.
899 61. Stokich B, Osgood Q, Grimm D, Moorthy S, Chakraborty N, Menze MA.
900 Cryopreservation of hepatocyte (HepG2) cell monolayers: impact of trehalose.
901 Cryobiology. 2014;69(2):281-90.
902

A.

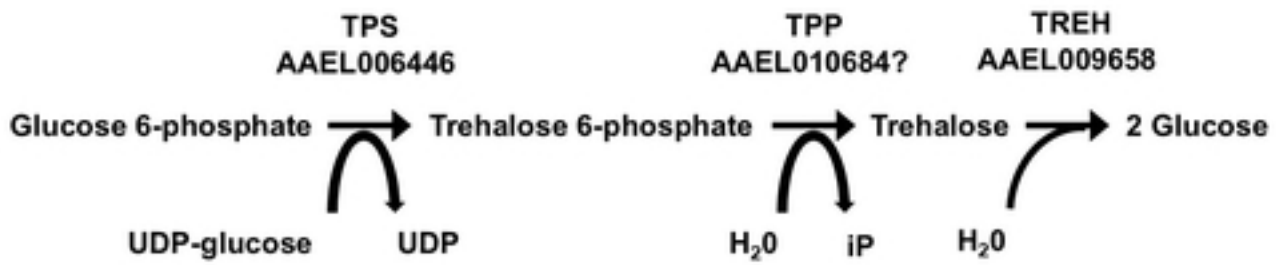
TPS
AAEL006446
TPP
AAEL010684?
TREH
AAEL009658
Glucose 6-phosphate
Trehalose 6-phosphate
Trehalose
2 Glucose
UDP-glucose
UDP
H_20
iP
H_20

B.

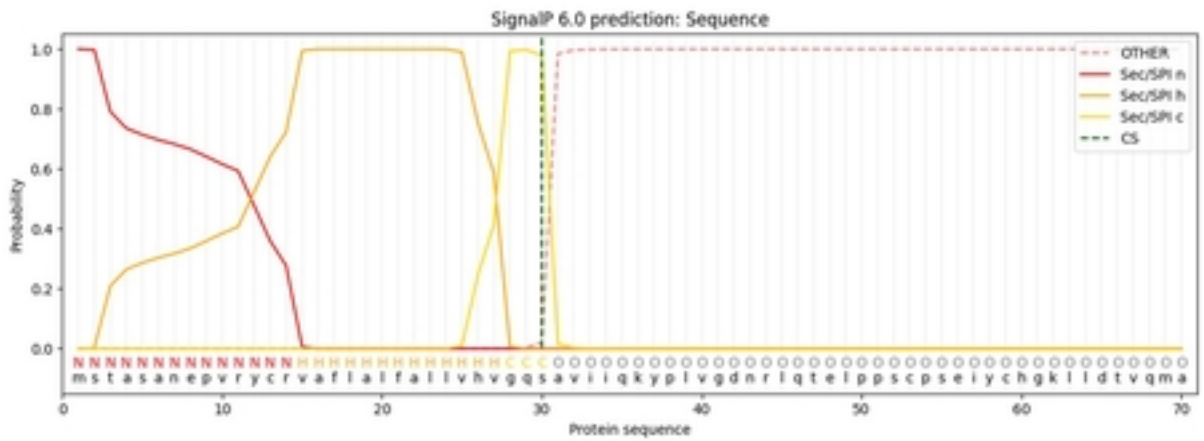
SignalP 6.0 prediction: Sequence
Probability
Protein sequence
OTHER
Sec/SPI n
Sec/SPI h
Sec/SPI c
CS

Figure 1

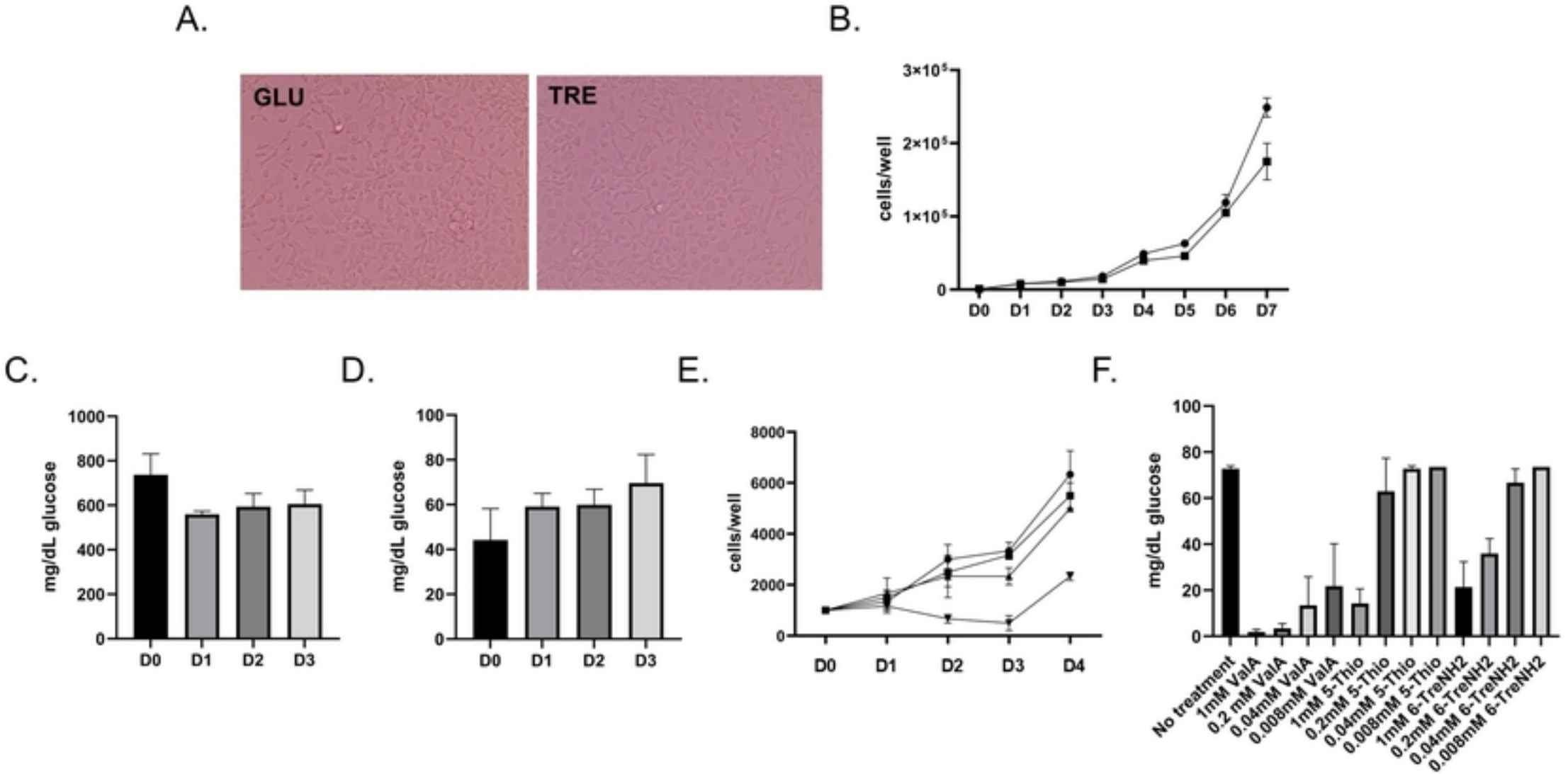
A.
GLU
TRE
B.
cells/well
3×10⁵
2×10⁵
1×10⁵
0
D0
D1
D2
D3
D4
D5
D6
D7
C.
mg/dL glucose
1000
800
600
400
200
0
D0
D1
D2
D3
D.
mg/dL glucose
100
80
60
40
20
0
D0
D1
D2
D3
E.
cells/well
8000
6000
4000
2000
0
D0
D1
D2
D3
D4
F.
mg/dL glucose
100
80
60
40
20
0
No treatment
1mM ValA
0.2 mM ValA
0.04mM ValA
0.008mM ValA
1mM 5-Thio
0.2mM 5-Thio
0.04mM 5-Thio
0.008mM 5-Thio
1mM 6-TreNH2
0.2mM 6-TreNH2
0.04mM 6-TreNH2
0.008mM 6-TreNH2

Figure 2

A.

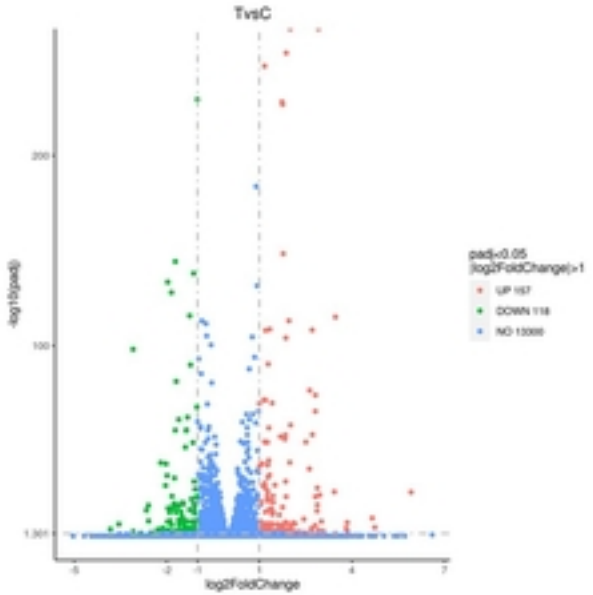

B.

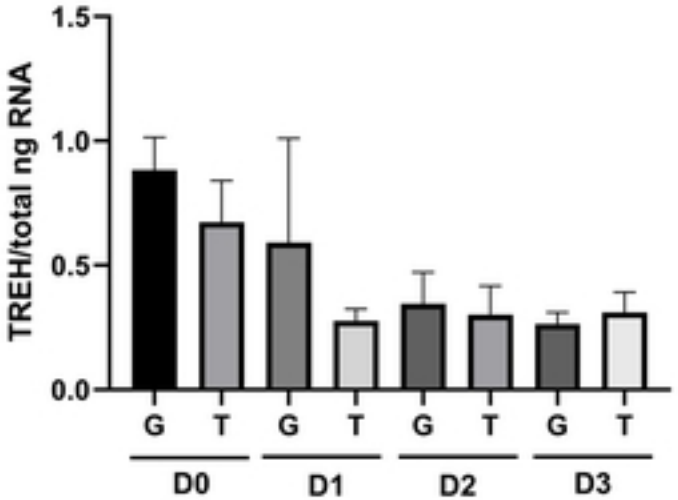

C.

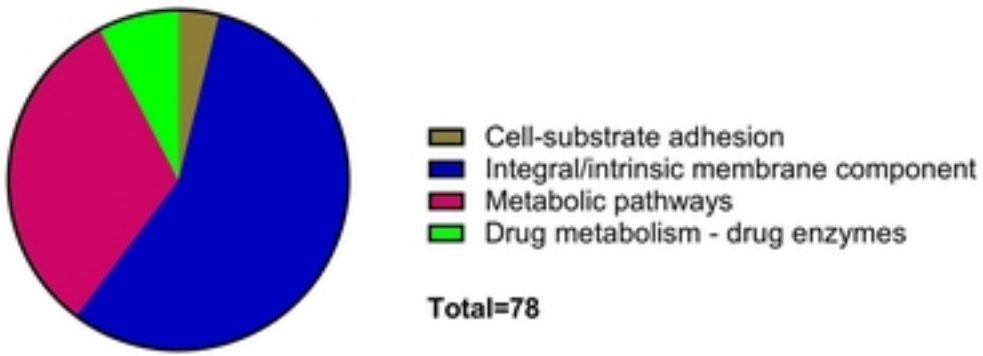

D.

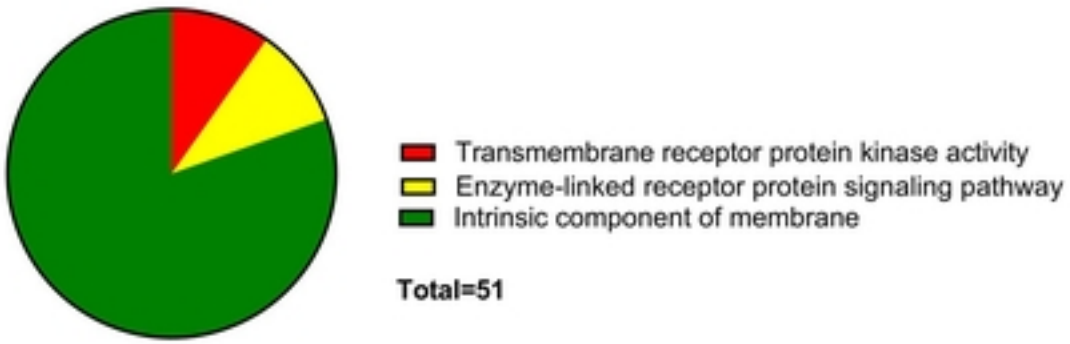

Figure 3

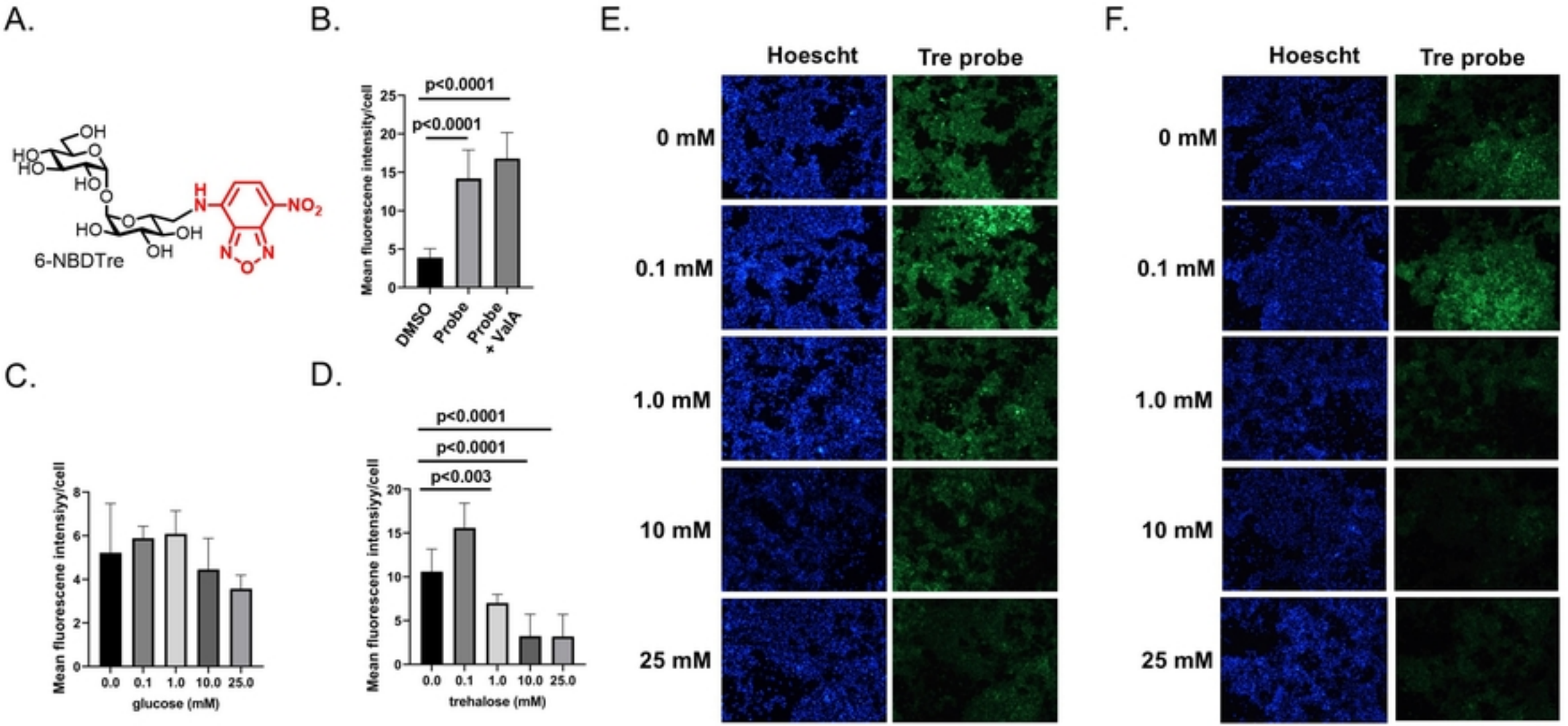
A.
6-NBDTre
B.
p<0.0001
p<0.0001
Mean fluorescene intensity/cell
DMSO
Probe
Probe + ValA
C.
Mean fluorescene intensiyy/cell
0.0
0.1
1.0
10.0
25.0
glucose (mM)
D.
p<0.0001
p<0.0001
p<0.003
Mean fluorescene intensiyy/cell
trehalose (mM)
E.
Hoescht
Tre probe
0 mM
0.1 mM
1.0 mM
10 mM
25 mM
F.
Hoescht
Tre probe
0 mM
0.1 mM
1.0 mM
10 mM
25 mM

Figure 4

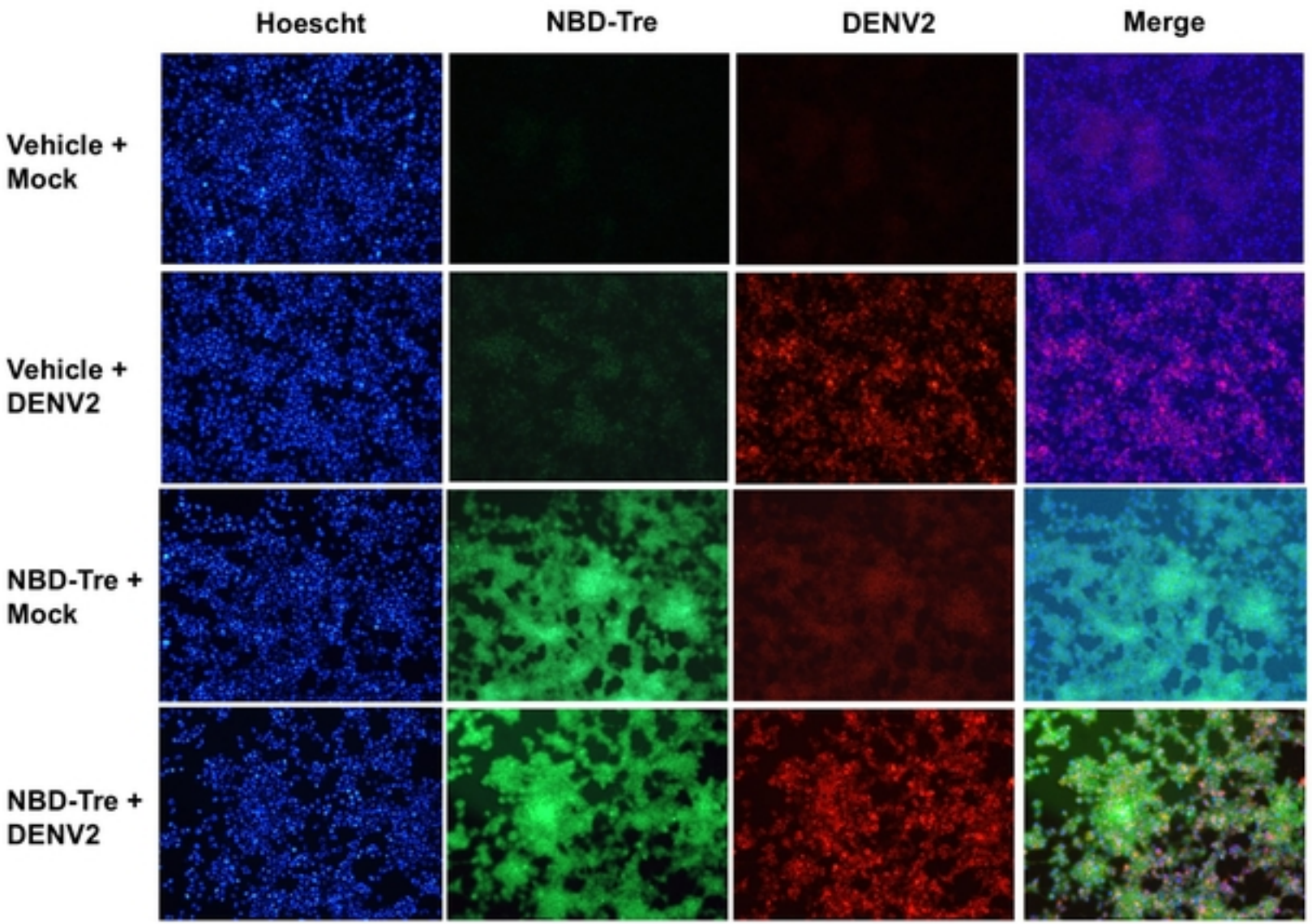
Hoescht
NBD-Tre
DENV2
Merge
Vehicle + Mock
Vehicle + DENV2
NBD-Tre + Mock
NBD-Tre + DENV2

Figure 5

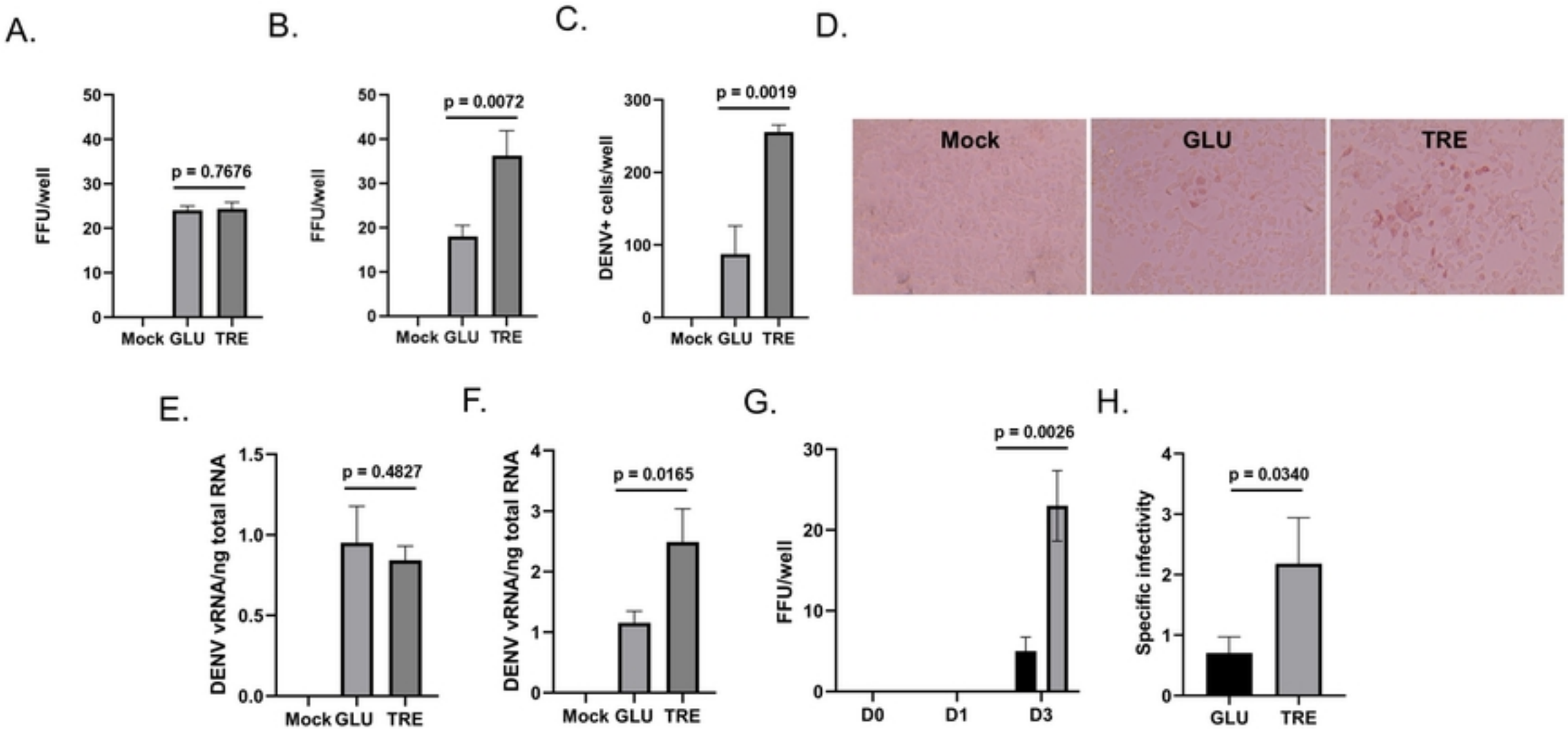
A.
FFU/well
p = 0.7676
Mock GLU TRE
B.
FFU/well
p = 0.0072
Mock GLU TRE
C.
DENV+ cells/well
p = 0.0019
Mock GLU TRE
D.
Mock
GLU
TRE
E.
DENV vRNA/ng total RNA
p = 0.4827
Mock GLU TRE
F.
DENV vRNA/ng total RNA
p = 0.0165
Mock GLU TRE
G.
FFU/well
p = 0.0026
D0 D1 D3
H.
Specific infectivity
p = 0.0340
GLU TRE

Figure 6

A.

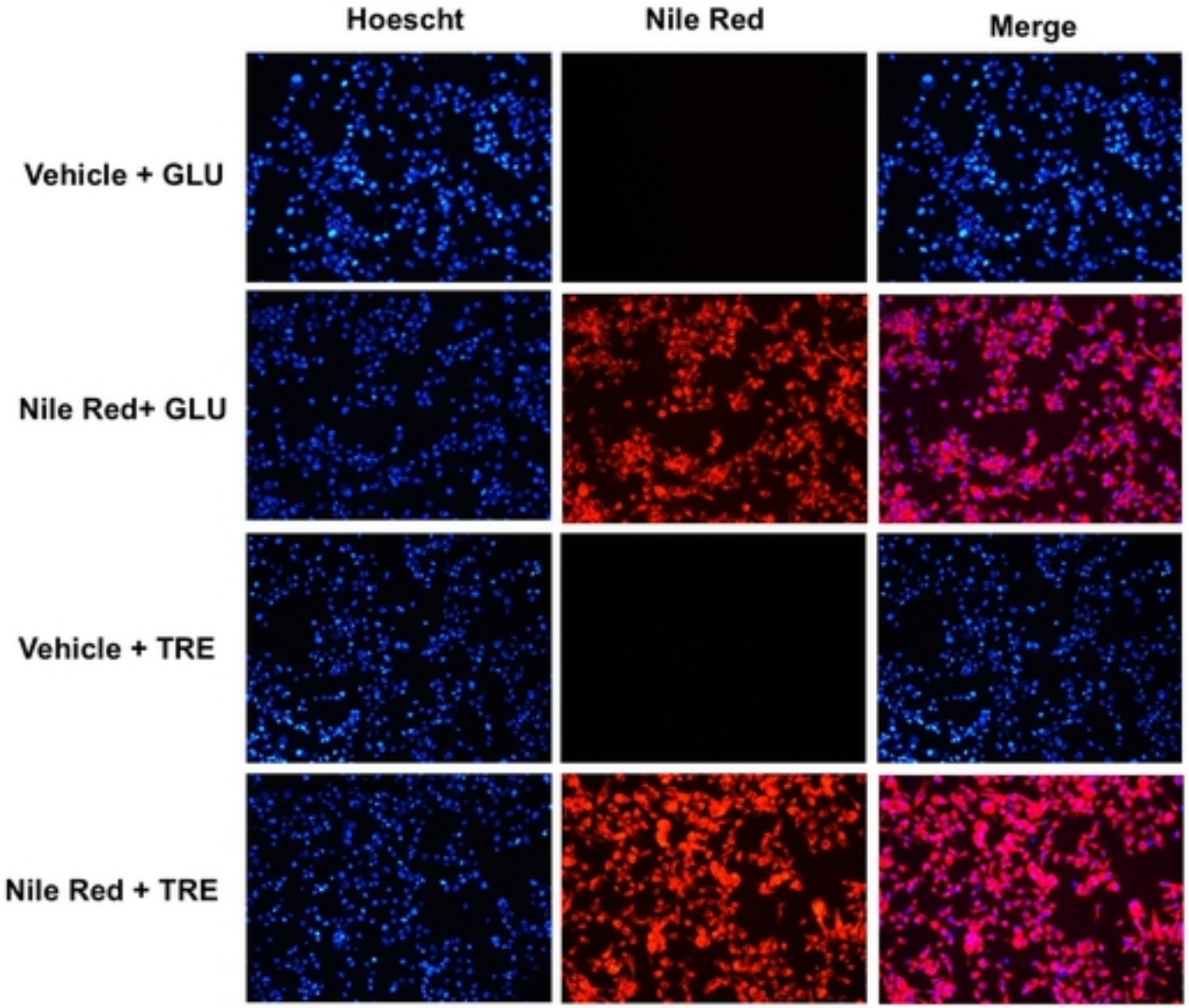
Hoescht
Nile Red
Merge
Vehicle + GLU
Nile Red+ GLU
Vehicle + TRE
Nile Red + TRE

B.

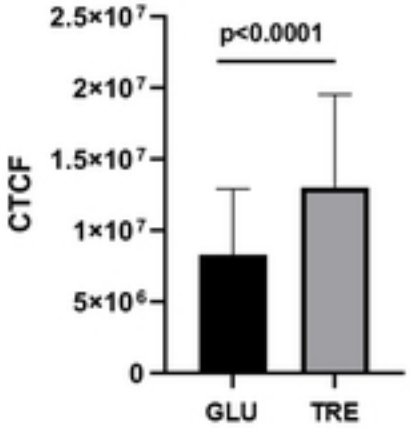
p<0.0001
CTCF
2.5×10⁷
2×10⁷
1.5×10⁷
1×10⁷
5×10⁶
0
GLU
TRE

Figure 7

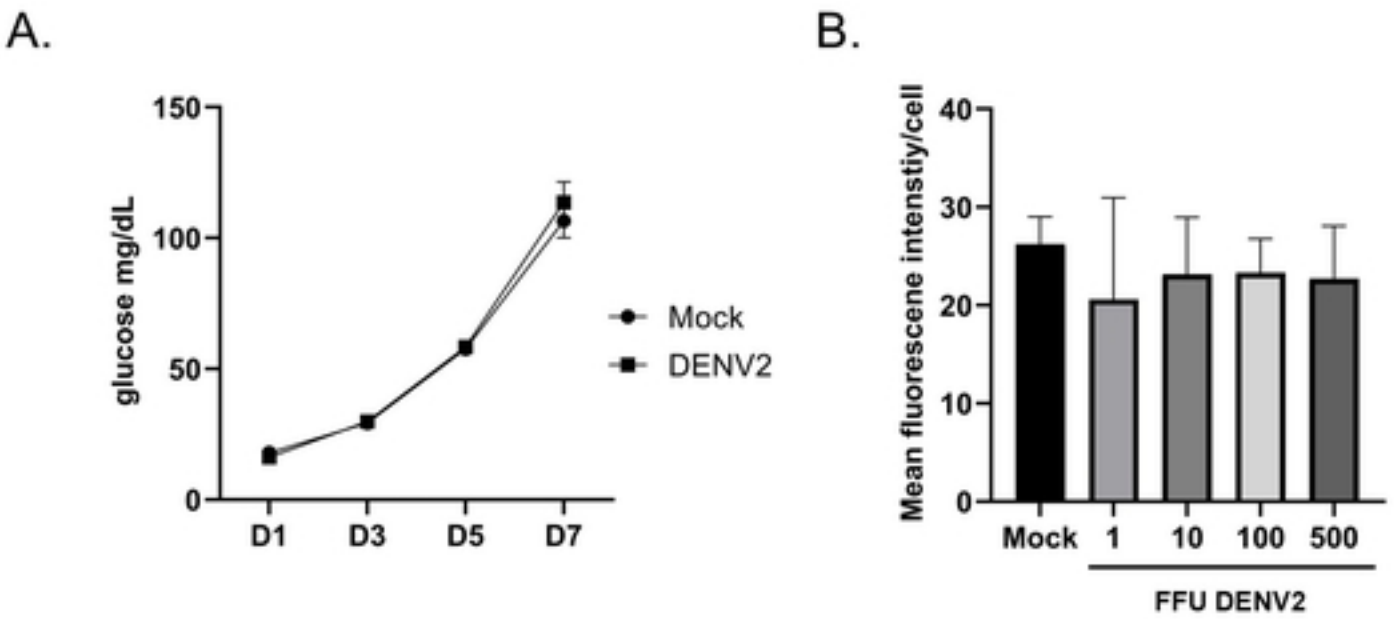
A.
150
100
50
0
glucose mg/dL
D1
D3
D5
D7
Mock
DENV2
B.
40
30
20
10
0
Mean fluorescene intenstiy/cell
Mock
1
10
100
500
FFU DENV2

Figure 8

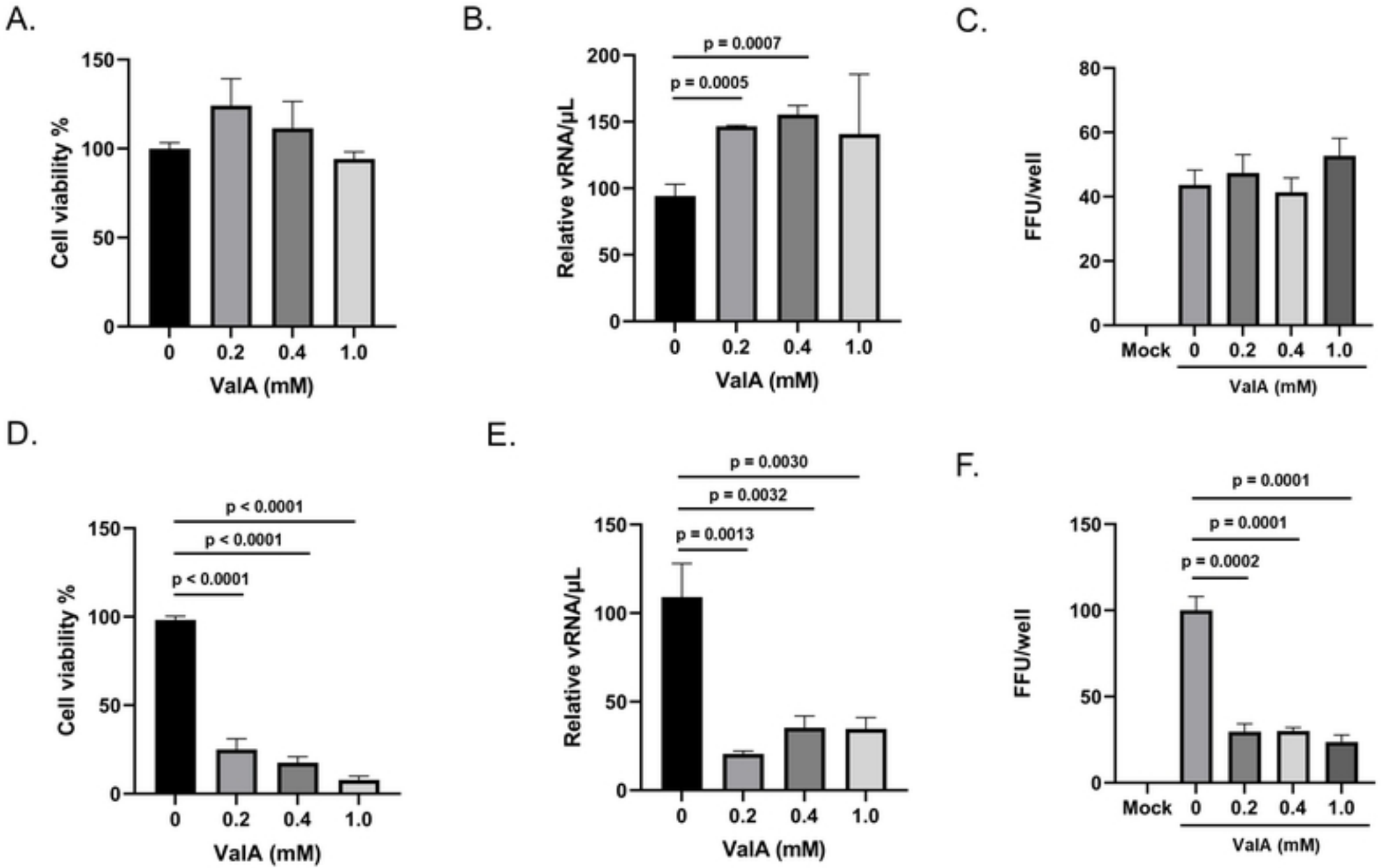
A.
Cell viability %
150
100
50
0
0
0.2
0.4
1.0
ValA (mM)
B.
Relative vRNA/µL
200
150
100
50
0
p = 0.0007
p = 0.0005
0
0.2
0.4
1.0
ValA (mM)
C.
FFU/well
80
60
40
20
0
Mock
0
0.2
0.4
1.0
ValA (mM)
D.
Cell viability %
150
100
50
0
p < 0.0001
p < 0.0001
p < 0.0001
0
0.2
0.4
1.0
ValA (mM)
E.
Relative vRNA/µL
150
100
50
0
p = 0.0030
p = 0.0032
p = 0.0013
0
0.2
0.4
1.0
ValA (mM)
F.
FFU/well
150
100
50
0
p = 0.0001
p = 0.0001
p = 0.0002
Mock
0
0.2
0.4
1.0
ValA (mM)

Figure 9